



# OPEN Menstrual blood-derived stem cell exosomes improve ovarian function in chemotherapy-Induced POF rats via apoptosis regulation

Xianying Cheng<sup>1,8</sup>, Yanqin Wu<sup>1,8</sup>, Li Cheng<sup>2,8</sup>, Minjie Liu<sup>3</sup>, Kwanghann Gan<sup>1</sup>,  
Yuanyuan Wang<sup>4</sup>, Ting Zhang<sup>5</sup>, Lingqiao Yang<sup>6</sup>, Yige Wang<sup>7</sup>, Liya Xu<sup>1</sup>✉ & Zhenyu Xu<sup>7</sup>✉

Recent studies have demonstrated that exosome therapy can promote the recovery of ovaries in premature ovarian failure (POF) models, which may aid in fertility restoration. This study aimed to investigate the therapeutic efficacy of exosomes derived from menstrual blood-derived mesenchymal stem cells (MenSCs-Exos) in a POF rat model, exploring its underlying mechanisms and detecting the optimal effective therapeutic dose. A POF model was established by an alkylating agent cyclophosphamide (CTX). All POF rats were divided into four groups (eight rats per group) and received a single intervention via the tail vein: phosphate-buffered saline (PBS), low-dose MenSCs-Exos (0.5 mL), middle-dose MenSCs-Exos (1 mL), high-dose MenSCs-Exos (2.0 mL). The concentration of MenSCs-Exos was  $1 \times 10^9$  particles/mL. Serum was collected from the tail vein before CTX injection and on the 14th day after MenSCs-Exos treatment to measure the serum levels of follicle-stimulating hormone (FSH), luteinizing hormone (LH), anti-Müllerian hormone (AMH), and estradiol (E<sub>2</sub>) via ELISA. The ovarian pathology and follicle counts were examined by H&E. The protein expression and concentration of B-cell lymphoma-2 (Bcl-2) and Bcl-2 associated X protein (Bax) in ovarian tissue were examined by western blot and ELISA. Rats in the middle- and high-dose MenSCs-Exos groups recovered their physical condition after treatment, and their body weight was significantly higher than that of the placebo group but lower than that of the control group, respectively ( $P < 0.05$ ). Compared to the placebo group, serum E<sub>2</sub> and AMH levels were significantly increased, while serum FSH and LH levels were decreased ( $P < 0.05$ ). MenSCs-Exos treatment also improved ovarian tissue morphology, and the number of follicles at all stages was markedly increased compared with those in the placebo group ( $P < 0.05$ ). In addition, the expression of anti-apoptotic Bcl-2 protein was significantly up-regulated and the expression of pro-apoptotic Bax protein was markedly inhibited after treatment, and the Bcl-2/Bax ratio was also significantly increased ( $P < 0.05$ ). Finally, the middle-dose achieved optimal therapeutic effect among the three MenSCs-Exos groups, as the low-dose achieved a less effective outcome and the high-dose exerted no additional therapeutic effects. MenSCs-Exos transplantation could effectively restore ovarian function and promote ovarian regeneration in Chemotherapy-induced POF model, whose mechanism is mainly associated with the regulation of apoptotic-related proteins expression. Additionally, the effective dose is middle-dose MenSCs-Exos (1 mL) or  $1 \times 10^9$  particles in POF rats. Nevertheless, all these findings require further clinical validation in human models.

**Keywords** Premature ovarian failure, Chemotherapy, Menstrual blood-derived mesenchymal stem cells, Exosomes, Rat model

<sup>1</sup>Department of Obstetrics and Gynecology, Shulan (Hangzhou) Hospital, Shulan International Medical College, Zhejiang Shuren University, Hangzhou 310022, China. <sup>2</sup>Department of Obstetrics and Gynecology, Hangzhou Xixi Hospital, Hangzhou 310023, China. <sup>3</sup>Clinical Laboratory, Shulan (Hangzhou) Hospital, Shulan International Medical College, Zhejiang Shuren University, Hangzhou 310022, China. <sup>4</sup>Department of Obstetrics and Gynecology, The Affiliated Hospital of Hangzhou Normal University, Hangzhou 310015, China. <sup>5</sup>Department of Pathology, Shulan (Hangzhou) Hospital, Shulan International Medical College, Zhejiang Shuren University, Hangzhou 310022, China. <sup>6</sup>Cellular Therapy Drugs R&D Center, Innovative Precision Medicine (IPM) Group, Hangzhou 311217, China. <sup>7</sup>Cellular Therapy Drugs Innovation Research Institute, Innovative Precision Medicine (IPM) Group, Hangzhou 311217, China. <sup>8</sup>These are contributed equally to this work: Xianying Cheng, Yanqin Wu and Li Cheng. ✉email: 826015411@qq.com; dannyxu@ipmbiotech.com

Premature ovarian failure (POF) is a complex multifactorial disorder affecting women under the age of 40, with significant physiological and psychological implications<sup>1</sup>. The incidence of POF is 1 in 100 women before 40 years of age and 1 in 1000 women before 30 years of age<sup>2</sup>. Although the precise pathogenic mechanisms of POF remain unclarified and is associated with multiple complicated factors, including genetic disorders, iatrogenic factors, autoimmunity and environmental and infectious factors. Chemotherapy-induced ovarian damage is one of the leading causes of iatrogenic POF in cancer patients, which has drawn growing concern among females with fertility needs in recent years<sup>3</sup>. Until now, hormone replacement therapy is the mainstay of management. However, this kind of treatment can only relieve related symptoms but cannot restore ovarian function and fertility fundamentally<sup>4</sup>. The most common approach for POF women to fulfill reproductive involves the utility of donated oocytes from other women in clinical practice<sup>5</sup>, but oocyte donation resources are very scarce<sup>6</sup>. Therefore, it is urgent to explore effective therapeutic solutions for women with POF diagnosed with infertility in the field of reproductive medicine.

Recently, mesenchymal stem cells (MSCs) research and therapy have brought hope for various refractory diseases, which can restore ovarian function and improve fertility damage caused by chemotherapy<sup>7,8</sup>. However, the clinical application of MSCs is often associated with notable limitations, including safety concerns, limited sources, thromboembolism risk, poor in vivo survival rate, and immune rejection, which further constrains their clinical utility. Fortunately, a type of extracellular vesicles derived from MSCs called exosomes can overcome MSCs' drawbacks, which have the same efficacy in tissue regeneration and injury restoration as their source cells<sup>9</sup>. Exosomes are biocompatible, stable, low-toxic, and non-immunogenic when compared with MSCs, making them a novel cell-free therapeutic agent<sup>10</sup>. A systematic review and meta-analysis of clinical trials has also shown that exosomal therapy is safe, with a low incidence of serious and non-serious adverse events<sup>11</sup>. Therefore, exosomes may be a prospective cell-free substitute for MSCs as a strategy for treating POF. Actually, exosomes derived from amniotic fluid mesenchymal stem cells (AFSCs) and bone marrow mesenchymal stem cells (BMSCs) were demonstrated to restore ovarian function in a POF mouse model through the proteins and RNAs that they contain<sup>12,13</sup>.

Menstrual blood-derived mesenchymal stem cells (MenSCs) possess comprehensive advantages, including periodic and non-invasive sampling, continuous donor availability, superior proliferative capacity, and ample sources<sup>14</sup>, which ensure the sustainable and facile isolation of exosomes from MenSCs<sup>15</sup>. Furthermore, healthy donors can provide large quantities of MenSCs-Exos with a stable genetic background and consistent biological activity, which not only meets the quantitative requirements for clinical application but also guarantees the quality of exosomes for exosome-based therapy. Thereby, MenSCs-Exos hold great promise as a cell-free substitute for MenSCs as a strategy for the treatment of POF. In our study, we aimed to evaluate how exosomes derived from menstrual blood-derived mesenchymal stem cells (MenSCs-Exos) transplantation restore ovarian function and promote ovarian tissue regeneration in a POF model induced by cyclophosphamide (CTX), and the underlying mechanism. Previous literatures have shown that exosomes derived from different tissues have restored ovarian function in POF models. However, no published studies have investigated its dose-dependent therapeutic effects, so we simultaneously evaluated the efficacy of different therapeutic doses of MenSCs-Exos in this study. Our findings identify a novel bioresource-based cell-free therapeutic strategy that has the potential to restore ovarian function and improve reproductive health in patients with POF.

## Materials and methods

### Culture and identification of MenSCs

MenSCs were isolated from menstrual blood collected using a menstrual cup on the second day of the menstrual cycle. The inclusion criteria were healthy premenopausal women aged under 40 years with regular menstrual cycles who had not received any hormonal therapy.

The MenSCs were isolated and cultured to passage 5, and detailed identification methods were described in a previous study<sup>16</sup>. In short, MenSCs were isolated from menstrual blood samples and cultured in DMEM/F12 medium containing 10% fetal bovine serum at 37 °C and in an atmosphere with 5% CO<sub>2</sub>. The culture medium was changed every 3 days. Cells of passage 5 (P5) were collected, and cell surface markers (positive for CD29, CD44, CD73, CD90, and CD105; negative for CD34 and CD45) were identified via flow cytometry.

### Ethics statement

All animal study protocols were approved by the Ethics Committee of the Zhejiang Experimental Animal Center (ZJCLA-IACUD-20010032). All animal experiments complied with the ARRIVE guidelines and were

carried out in accordance with the UK Animals (Scientific Procedures) Act, 1986 and associated guidelines, EU Directive 2010/63/EU for animal experiments, and the National Institutes of Health guide for the care and use of Laboratory animals (NIH Publications No. 8023, revised 1978). Menstrual blood collection was approved by the Ethics Committee of Shulan (Hangzhou) Hospital (KY2022031) and was performed in accordance with the principles of the Declaration of Helsinki. All donors gave written informed consent for MenSCs collection and isolation.

### Extraction and identification of MenSCs-Exos

MenSCs-Exos were extracted from the culture supernatant using proprietary technology of the Innovative Precision Medicine (IPM) Group (Patent ID: CN202210193450). Briefly, exosomes were extracted and purified via three sequential steps: clarification, tangential flow ultrafiltration (flow rate: 2.5 mL/min; membrane pore size: 0.22  $\mu$ m), and affinity chromatography. The final particle concentration of the purified exosomes was  $1 \times 10^{10}$  particles/mL. The morphology of MenSCs-Exos was observed under a transmission electron microscope (TEM) and exhibited a particle size range of 30–150 nm. Briefly, 10  $\mu$ L of exosome suspension was placed on a Formvar-carbon-coated grid (400 meshes) and air-dried for 20 min at room temperature. Subsequently, the grids were rinsed with phosphate-buffered saline (PBS) and fixed with 1% glutaraldehyde for 5 min, rinsed again with deionized water, and negatively stained with uranyl oxalate for 5 min. After drying, the microstructure of exosomes was observed and imaged by a transmission electron microscope (talos120, FEI, USA) at 120 kV.

The size distribution and particle concentration of exosomes were measured by a Nano-Flow cytometry (U30, NanoFCM Inc, Xiamen, China). The instrument was calibrated for particle concentration using 250 nm SiNPs beads and for size distribution using Silica Nanosphere Cocktail (S16M-Exo (68, 91, 113, 155 nm) to make particle size modes were Gaussian-distributed and beads matched exosome refractive index. All the particles passing through the detector were recorded during a 1 min interval. Samples were diluted in PBS at an appropriate dilution ratio (1:150–200) and then loaded under a controlled flow at a pressure of 1.0 kPa. The size distribution and particle concentration data were analyzed by the NanoFCM Software V1.17, whose gating strategy used was a 488 nm laser (NanoFCM Inc, Xiamen, China)<sup>16</sup>.

Specific surface markers (e. g. , CD9, CD63, CD81) were identified via Nano-Flow cytometry, which involved labeling with fluorophore-conjugated specific antibodies against CD9 (12A12, Cosmo Bio, China), CD63 (8A12, Cosmo Bio, China), and CD81 (12C4, Cosmo Bio, China). Isolated exosomes bound to these surface marker samples were prepared and analyzed by Nano-Flow cytometry to determine the presence and quantity of the labeled surface markers, including size, concentration qualification and validation of CD9, CD63 and CD81 presence of MenSCs-Exos<sup>16</sup>. Unbound antibodies were removed prior to flow cytometric analysis. Isotype controls were used to verify the specificity of the assay, and exosomes were negative for hematopoietic markers (e. g. , CD34, CD45).

### Chemicals and antibodies

The information of primary reagents and antibodies can be seen in Table 1.

### Animal experimental procedures

The rats were purchased from Hangzhou Ziyuan experimental animal Technology Co. , Ltd. (China) SCXK (Zhejiang) 2019–0004. Forty female Sprague Dawley (SD) rats with regular estrous cycles (9–10 weeks old, body weight  $180 \pm 20$  g) were used in this study and housed in the Animal Experiment Center of the First Affiliated Hospital of Zhejiang University School of Medicine under controlled conditions (temperature:  $22 \pm 2$  °C; relative humidity:  $40 \pm 60\%$ ). Five rats were housed per cage with ad libitum access to food and water, and exposed to a 12 h light/12 h dark cycle. Food, water, bedding, and cages were strictly sterilized.

After 1 week of acclimatization, 32 SD rats were randomly selected using a random number table and received a single intraperitoneal injection of CTX (120 mg/kg) dissolved in 0.9% normal saline to establish the POF model (CTX group)<sup>17</sup>. Eight additional rats served as the control group and received an equivalent volume of PBS via intraperitoneal injection. All experiments were performed by blinded investigators to avoid

Antibody or ELISA kit	Catalog numbers	Producer	Location
Follicle stimulating hormone (FSH)	JM-02711R1	Jingmei Biotechnology Co., Ltd	China
Luteinizing hormone (LH)	JM-10711R1	Jingmei Biotechnology Co., Ltd	China
Anti-mullerian hormone (AMH)	JM-02731R1	Jingmei Biotechnology Co., Ltd	China
Estradiol(E2)	JM-02730R1	Jingmei Biotechnology Co., Ltd	China
B-cell lymphoma-2(Bcl-2)	JM-02721R1	Jingmei Biotechnology Co., Ltd	China
Bcl-2 associated X protein (Bax)	JM-13742R1	Jingmei Biotechnology Co., Ltd	China
Bcl-2 monoclonal antibody	B3781	Shanghai Guangrui Biotechnology Co., Ltd	China
Bax monoclonal antibody	B3771	Shanghai Guangrui Biotechnology Co., Ltd	China
Cyclophosphamide (CTX)	H32020856	Hengrui Pharmaceuticals Co., Ltd	China
Enhanced chemiluminescence (ECL)	B2521	Shanghai Guangrui Biotechnology Co., Ltd	China
DMEM/F12 medium	CM-A201001	BioInno Bioscience Co., Ltd	China
phosphate-buffered saline (PBS)	KL-25-160,129	Shanghai Kanglang Biotechnology Co., LTD	China

**Table 1.** The information of primary reagents and antibodies.

bias in outcome assessment. Vaginal smears were collected for 7 consecutive days starting from the 8th day after injection. Vaginal exfoliated cell smear examination was performed at 9 a. m. daily to assess the estrous cycle of rats. A sterile cotton swab was soaked in normal saline, inserted 1–2 cm into the rat's vagina, and rotated clockwise along the vaginal wall 1–2 times; the exfoliated vaginal cells were then spread on a glass slide. After air-drying for 1 min, the slide was stained with methylene blue solution for 15 min, rinsed three times with distilled water, and observed under a light microscope. The morphological characteristics of proestrus, estrus, metestrus, and diestrus were recorded. Estrous cycle disorder indicated that the POF model had been successfully established. Two weeks after CTX injection, the 32 POF rats were randomly divided into four groups (eight rats per group): the placebo group received 1 mL of PBS via tail vein injection; the low-, middle-, and high-dose exos groups received 0.5, 1, and 2 mL of MenSCs-Exos, respectively. The normal control group also received 1 mL of PBS via tail vein injection at the same time. MenSCs-Exos were resuspended in PBS to a final concentration of  $1 \times 10^9$  particles/mL, and all injections were performed via the tail vein using a microinjector.

Blood samples were collected from the tail vein before CTX injection and on the 14th day after MenSCs-Exos treatment. After 14 days of treatment, the animals were euthanized with sodium pentobarbital, and additional blood samples were collected via abdominal aortic puncture. All blood samples were incubated at room temperature for 2 h, centrifuged at 3000 rpm for 15 min, and the supernatant (serum) was collected and stored at  $-80^\circ\text{C}$  until analysis. Serum hormone concentrations were measured via commercial ELISA kits.

### Hormone determination

The concentration of the hormone was determined by ELISA kits. According to the manufacturer's instructions, rat FSH, LH, AMH, and E2 standards were diluted in the kit-provided standard diluent to the following final concentrations: 0, 5.0, 10, 20, 40, 80 pmol/L (FSH); 0, 1.5, 3, 6, 12, 24 mIU/mL (LH); 0, 1.5, 3, 6, 12, 24 mIU/mL (AMH); and 12.5, 25, 50, 100, 200 pg/mL (E2).

50  $\mu\text{L}$  of standard solution was added to precoated microtiter wells, and 10  $\mu\text{L}$  of serum was mixed with 40  $\mu\text{L}$  of sample diluent before loading into the wells. The plates were incubated for 30 min at  $37^\circ\text{C}$ . After five washing steps, 50  $\mu\text{L}$  of horseradish peroxidase (HRP)-conjugated secondary antibody was added, and the plates were incubated for an additional 30 min at  $37^\circ\text{C}$ . Tetramethylbenzidine (TMB) substrate was added to each well, the plates were sealed with a plastic film, and incubated at  $37^\circ\text{C}$  in the dark for 15 min. The optical density (OD) values of the samples were measured at 450 nm (reference wavelength: 570 nm). Serum hormone concentrations were calculated according to the standard curve generated for each assay.

### Histological analysis and ovarian follicle counting

Both ovaries were collected after aseptic laparotomy; one ovary was stored in an Eppendorf (EP) tube at  $-80^\circ\text{C}$ , and the other was fixed in 4% paraformaldehyde for at least 24 h. The fixed ovaries were dehydrated, embedded in paraffin, and serially sectioned at a thickness of 5  $\mu\text{m}$ ; the sections were stained with hematoxylin and eosin (H&E). The ovarian histological examination was performed using optical microscopy. Three ovarian sections were randomly selected per rat, and follicles were classified and counted across the entire section; the number of follicles at each stage across the three sections was summed for each rat. Histological assessment was performed by two independent blinded observers to ensure reproducibility. Follicles of every stage were detected and classified according to the description and criteria of the reference<sup>18</sup>. primordial follicles: oocytes surrounded by less differentiated squamous granulosa cells; primary follicles: oocytes surrounded by a single layer of cuboidal granulosa cells; secondary follicles: oocytes surrounded by two or more layers of cuboidal granulosa cells with no visible antrum; antral follicles: oocytes surrounded by five or more complete granulosa cell layers with a visible antrum.

### Western blot

Western blot analysis was performed according to standard laboratory protocols. Cryopreserved ovarian tissues were lysed in radioimmunoprecipitation assay (RIPA) buffer containing protease and phosphatase inhibitors, and total protein was extracted on ice for 30 min. Before sample loading, an appropriate volume of SDS-PAGE loading buffer was added to each protein sample. Protein concentrations were quantified using the bicinchoninic acid (BCA) assay, and equal amounts of total protein (10  $\mu\text{g}$  per lane) from each sample were separated by 10% SDS-PAGE at a constant voltage of 120 V for 60 min, then transferred to polyvinylidene fluoride (PVDF) membranes (Merck, Darmstadt, Germany) at a constant voltage of 65 V for 120 min. The PVDF membranes were blocked with 5% non-fat milk in TBST buffer at room temperature for 2 h. The membranes were incubated with primary antibodies at  $4^\circ\text{C}$  for 24 h: rabbit anti-mouse Bcl-2 (1:500, Abnova, MAB9756), rabbit anti-mouse Bax (1:100, LMAI Bio, LS-B1949), and rabbit anti-mouse  $\beta$ -actin (1:1000, LSBio, LS-C212188) ( $\beta$ -actin as the internal control). The membranes were washed with Tris-buffered saline with Tween 20 (TBST) buffer on a shaker at room temperature for 5 min per wash, for a total of four times. After primary antibody incubation and washing, the membranes were incubated with the HRP-labeled goat anti-rabbit IgG secondary antibody (1:500, Affinity Biosciences, S0001) at room temperature for 20 min. The membranes were again washed with TBST buffer on a shaker at room temperature for 5 min per wash, four times total. Equal volumes of Reagent A and B from a commercial high-sensitivity ECL detection kit were mixed in a clean tube to prepare the ECL working solution. The membrane was placed protein-side up, and ECL working solution was added dropwise to fully and evenly cover the membrane, followed by incubation at room temperature for 1–2 min. The membrane was blotted vertically on absorbent paper for a few seconds to remove excess ECL working solution. The membrane was immediately sealed between two layers of plastic wrap, and air bubbles between the membrane and plastic wrap were carefully removed. The membrane was placed protein-side up for exposure, then exposed to a chemiluminescence imager for 2 min. Blot images were captured and saved using a gel imaging analysis

system for quantification of relative Bcl-2 and Bax protein expression levels. All western blot experiments were independently repeated three times to ensure reproducibility.

### Ovarian tissue Bcl-2, Bax protein concentration determination

After thawing, ovarian tissues were rinsed with ice-cold PBS to remove residual blood, weighed, and minced into small pieces. The minced tissue and the corresponding volume of PBS (1:9, v/v) were added to a glass homogenizer, and the homogenate was fully ground on ice. Finally, the homogenate was centrifuged at  $5000 \times g$  for 5–10 min, and the supernatant was collected for subsequent analysis. The absorbance (OD) values of each well were measured at 450 nm wavelength on the ELISA kit in strict accordance with the instructions and procedures. With the OD value of the measured standard product as the horizontal coordinate and the concentration value of the standard product as the vertical coordinate, GraphPad Prism software was used to draw the standard curve, and the linear regression equation was obtained. The OD value of the sample was substituted into the equation to calculate the ovarian Bcl-2 and Bax protein concentrations.

Scheme of this experiment was shown in Fig. 1.

### Statistical analysis

One-way analysis of variance (ANOVA) was used for comparison of multiple groups, followed by Bonferroni correction for subsequent analysis. The normal distribution and homogeneity of variance were tested, and then paired t-tests were used for intragroup comparisons before and after treatment, and independent sample t-tests were used for comparison between two groups. All numerical values are presented as the mean  $\pm$  standard deviation (SD), and  $^*P < 0.05$ ,  $^{**}P < 0.01$  and  $^{***}P < 0.001$  were considered to indicate a statistically significant difference. All charts were generated using GraphPad Prism 10.1.2 software (San Diego, CA, USA) and statistical analyses were performed using SPSS 13.0 Statistical Analysis software (IBM SPSS Inc., Chicago, IL, USA).

## Results

### Characterization of MenSCs-Exos

AF647-CD9 and AF488-CD63 were markers on the surface of exosomes for identification by Nano-Flow cytometry, showing exosome populations with positive expression markers (Fig. 2A). FITC-CD81 is another surface marker (Fig. 2B).

The morphology of MenSCs-Exos can be visually seen through TEM, which exhibited a sphere-shaped and bilayer lipid vesicle with a diameter less than 150 nm (Fig. 2C). The size and concentration of MenSCs-Exos are shown in Fig. S1. Tetraspanin CD9, CD63 and CD81 were expressed positively on MenSCs-Exos. The size distribution of exosomes, which typically range from 30–150 nm, further confirmed the identity of exosomes.

### Intraperitoneal injection of CTX caused the rats' physical condition to deteriorate and led to hormonal disorder

The estrous cycle, activity, diet, excretion and hair shedding of rats were observed for 14 consecutive days during POF modeling. The rats' body weights were measured and recorded daily. The rats had bright hair color, no obvious hair loss, good responsiveness to external stimuli. The activity, water, diet and estrous cycle were normal in the control group. On the contrary, rats showed certain degrees of hair loss, dark and dull color, mental lethargy, slow response, loss of appetite, slow movement, estrous cycle disorder in the CTX group. The weight of rats in both groups showed an increasing trend during modeling (Fig. 3A), and there was a statistically significant difference between the control and CTX groups on day 1 before CTX injection and day 14 after injection. Furthermore, the weight gain of the control group was greater than that of the CTX group ( $P < 0.05$ , Fig. 3B). These results indicated that CTX could cause body functional damage to rats in some degrees.

Next, we evaluated the serum concentrations of FSH, LH,  $E_2$  and AMH on the 14th day after CTX injection. Compared to the control group, serum LH and FSH levels were significantly increased and AMH and  $E_2$  levels were decreased in the CTX group ( $P < 0.01$ , Fig. 3C). These results indicated that CTX caused serum hormones

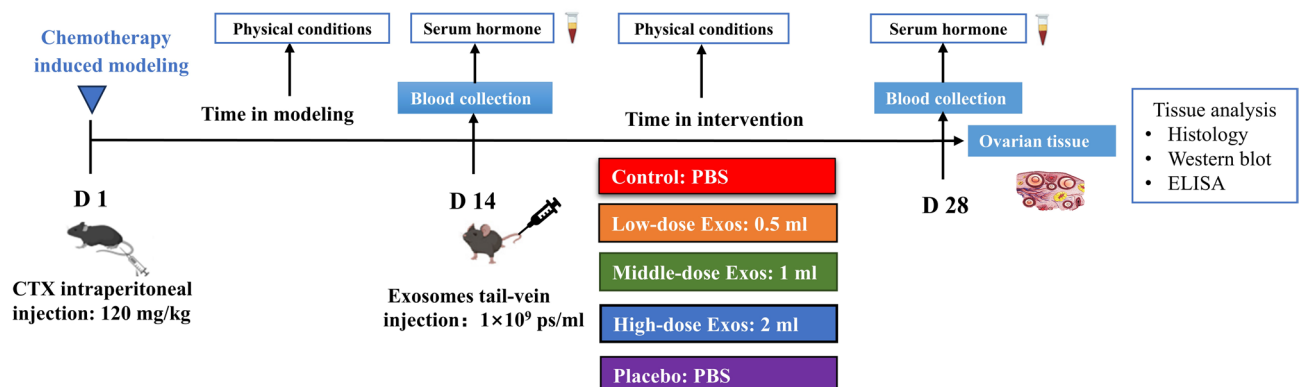
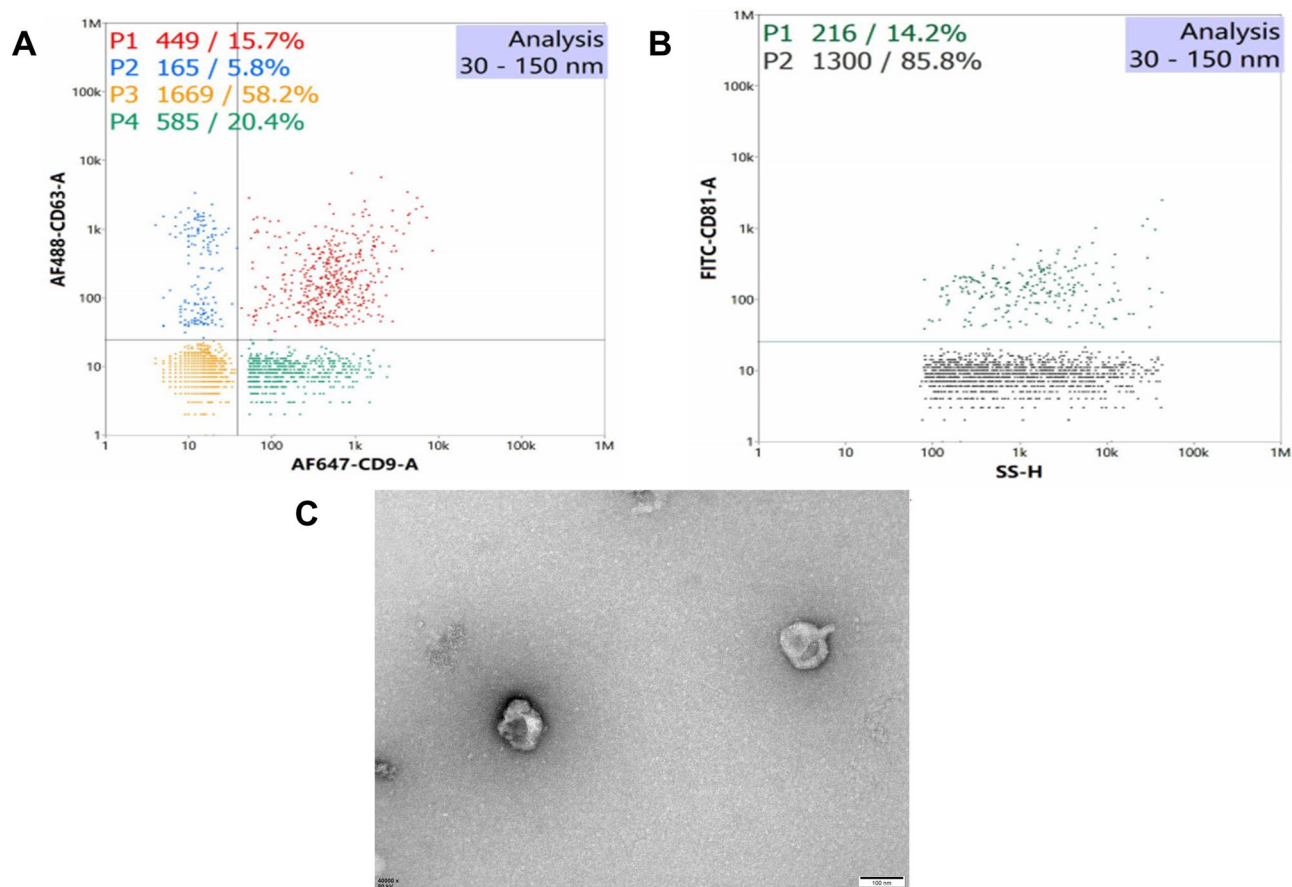


Fig. 1. Experimental procedure chart.



**Fig. 2.** The characterization of MenSCs-Exos. **(A):** Flow cytogram of CD9 and CD63. **(B):** Flow cytogram of CD81. **(C):** Morphology of MenSCs-Exos observed by TEM with a mean diameter of  $110 \pm 25$  nm (scale bar = 100 nm).

disorder. Therefore, combining with all the changes of physical condition and estrous cycle in the CTX group, it can be confirmed that the establishment of the POF model was successful.

### MenSCs-Exos transplantation restored physical condition and serum hormones in POF rats

After the POF rat model was established, 24 POF rats were randomly assigned to three groups and received tail-vein injections of different doses of MenSCs-Exos. Another eight rats received PBS via tail-vein injection as the placebo group. After that, the estrous cycle, activity, diet, excretion, hair shedding and weight of rats in all groups were continuously observed and recorded for 14 days. The weight of rats in all groups continued to show an increasing trend after treatment (Fig. 4A). Comparing with pre-treatment, rats in the middle-dose and high-dose MenSCs-Exos groups showed brighter hair color, less hair loss, better appetite, more activity, higher reaction agility, and restored regular estrous cycle, which achieved a similar result compared with the control group. However, the results did not show significant changes in the low-dose MenSCs-Exos and placebo groups after treatment.

ANOVA was used to compare body weight changes on the 14th day after treatment, and there was statistical significance among all five groups ( $F = 24.183$ ,  $P = 0.000$ ). Further pairwise comparisons revealed that the control group was significantly higher in body weight than the low-dose MenSCs-Exos and placebo groups, while no statistical significance between the control, middle-dose and high-dose MenSCs-Exos groups. It can be seen the same result between the low-dose MenSCs-Exos and placebo groups, middle-dose and high-dose MenSCs-Exos groups ( $P > 0.05$ , Fig. 4B). These results indicated that middle-dose or high-dose MenSCs-Exos transplantation ameliorated physical condition in POF rats which nearly recovered to normal state as the control group.

We further analyzed the serum concentrations of FSH, LH, AMH, and  $E_2$  to assess ovarian function after MenSCs-Exos transplantation. ANOVA showed that there was statistical significance in serum hormones concentrations among these five groups after fourteen-day's treatment. Serum LH and FSH levels were all increased in each treatment groups but AMH and  $E_2$  levels were decreased comparing with these in the control group ( $P < 0.05$ , Fig. 4C–F). Then we compared the levels of FSH, LH,  $E_2$  and AMH in the three transplantation groups, serum LH and FSH levels in the middle-dose and high-dose MenSCs-Exos groups were significantly decreased and  $E_2$  and AMH levels were increased comparing with the placebo group ( $P < 0.05$ , Fig. 4C–F). These results indicated that middle-dose and high-dose MenSCs-Exos transplantation both had a considerable restorative effect on the sex hormones in POF rats.

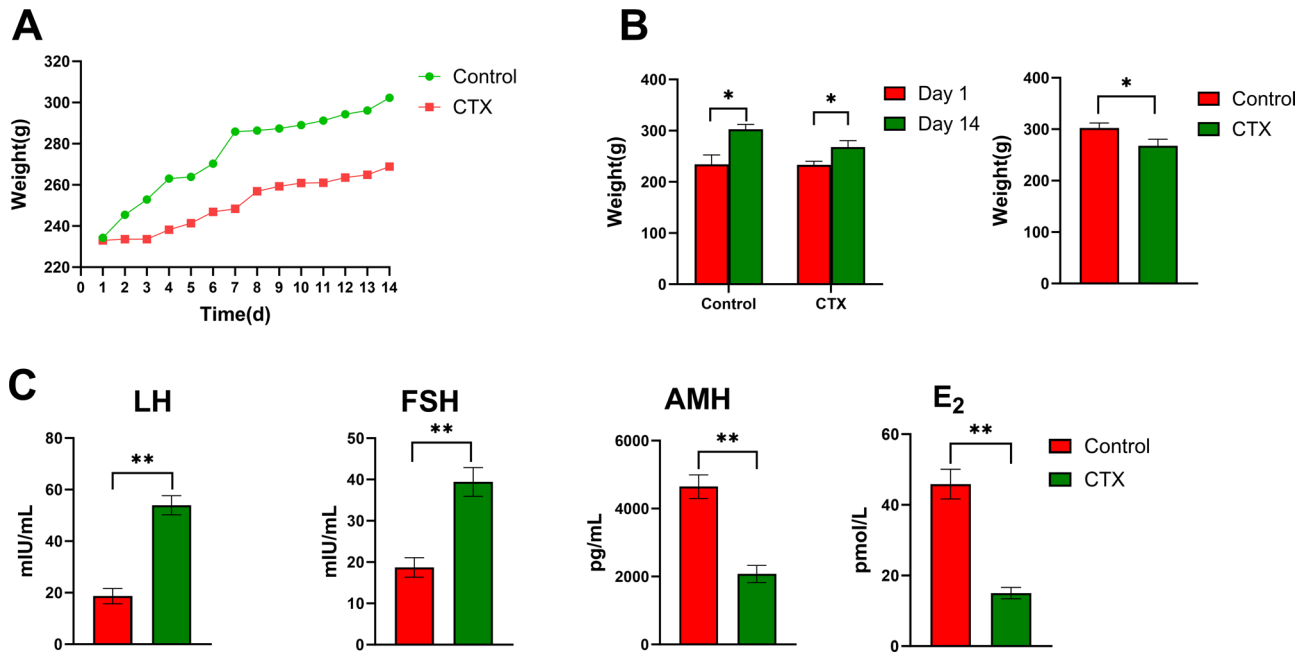


**Fig. 3.** Comparison of weight and serum sex hormones during modeling in the control and CTX groups. **(A):** Trend of weight changes during modeling in the control and CTX groups. **(B):** Comparison of weight on day 1 and day 14 between the control and CTX groups after modeling. **(C):** Comparison of serum sex hormones between the control and CTX groups after modeling. Data were represented as mean  $\pm$  SD, \* $P < 0.05$ , \*\* $P < 0.01$ .

### MenSCs-Exos transplantation improved ovarian morphology and promoted follicle development in POF rats

The size and weight of ovaries were lower in the low-dose MenSCs-Exos and placebo groups compared with the other groups. H&E staining showed that the ovarian histomorphology was clear in the control group, with abundant follicles at all stages developing normally and the granulosa cell layers arranged regularly. A certain number of primordial, primary, secondary, and antral follicles, fewer atretic follicles, relative regular arrangement of granulosa cells and fibrotic alterations in part of the ovarian stroma were observed in the middle-dose group. Similar results were found in the high-dose group. By contrast, the low-dose and placebo groups showed ovarian atrophy, disordered structures, reduced the number of follicles, increased atretic follicles, decreased granulosa cells with loose and disordered arrangement, abnormal nuclear morphology in some cells, reduction of ovarian blood vessel, and the interstitial increased (Fig. 5A).

Further follicle counts indicated that there were significant differences in all types of follicles among five groups on the 14th day after MenSCs-Exos transplantation. The number was distinctly decreased in the four treatment (low-dose, mid-dose, high-dose, placebo) groups comparing with the control group ( $P < 0.05$ , Fig. 5B–E). And it was increased in the middle-dose and high-dose MenSCs-Exos groups compared with the low-dose MenSCs-Exos group. These results revealed that middle-dose and high-dose MenSCs-Exos transplantation both improved ovarian tissue morphological damage caused by CTX and promoted follicles development in POF rats.

### MenSCs-Exos transplantation up-regulated Bcl-2 and down-regulated Bax

Based on the above results, to further verify the potential mechanism of MenSCs-Exos in treating POF, we conducted western blot to determine the expression of apoptotic-related proteins (Fig. 6A). The findings confirmed that the expression of the anti-apoptotic Bcl-2 protein was significantly upregulated, and the pro-apoptotic Bax protein was markedly downregulated in the middle- and high-dose groups after MenSCs-Exos transplantation compared with the placebo group ( $P < 0.05$ , Fig. 6B, C).

Meanwhile, we determined Bcl-2 and Bax protein concentrations in ovarian tissue by ELISA. The results showed the concentration of Bcl-2 protein was significantly higher, and that of Bax protein was lower, in the middle- and high-dose MenSCs-Exos groups than in the low-dose MenSCs-Exos and placebo groups ( $P < 0.05$ , Fig. 6D, E). The Bcl-2/Bax ratio in the middle-dose and high-dose MenSCs-Exos groups were higher than these in the low-dose MenSCs-Exos and placebo groups ( $P < 0.05$ , Fig. 6F). The above results indicated MenSCs-Exos may improve ovarian function and promote follicle development by regulating apoptotic-related protein expression.

### Discussion

Over the last decade, MSCs transplantation was found to be a promising therapy for POF patients<sup>19,20</sup>. However, there are many shortcomings of MSCs therapy which constraint extensive clinical application. Exosomes are extracellular vesicles with a diameter of 30–150 nm that contain various biologically active molecules and

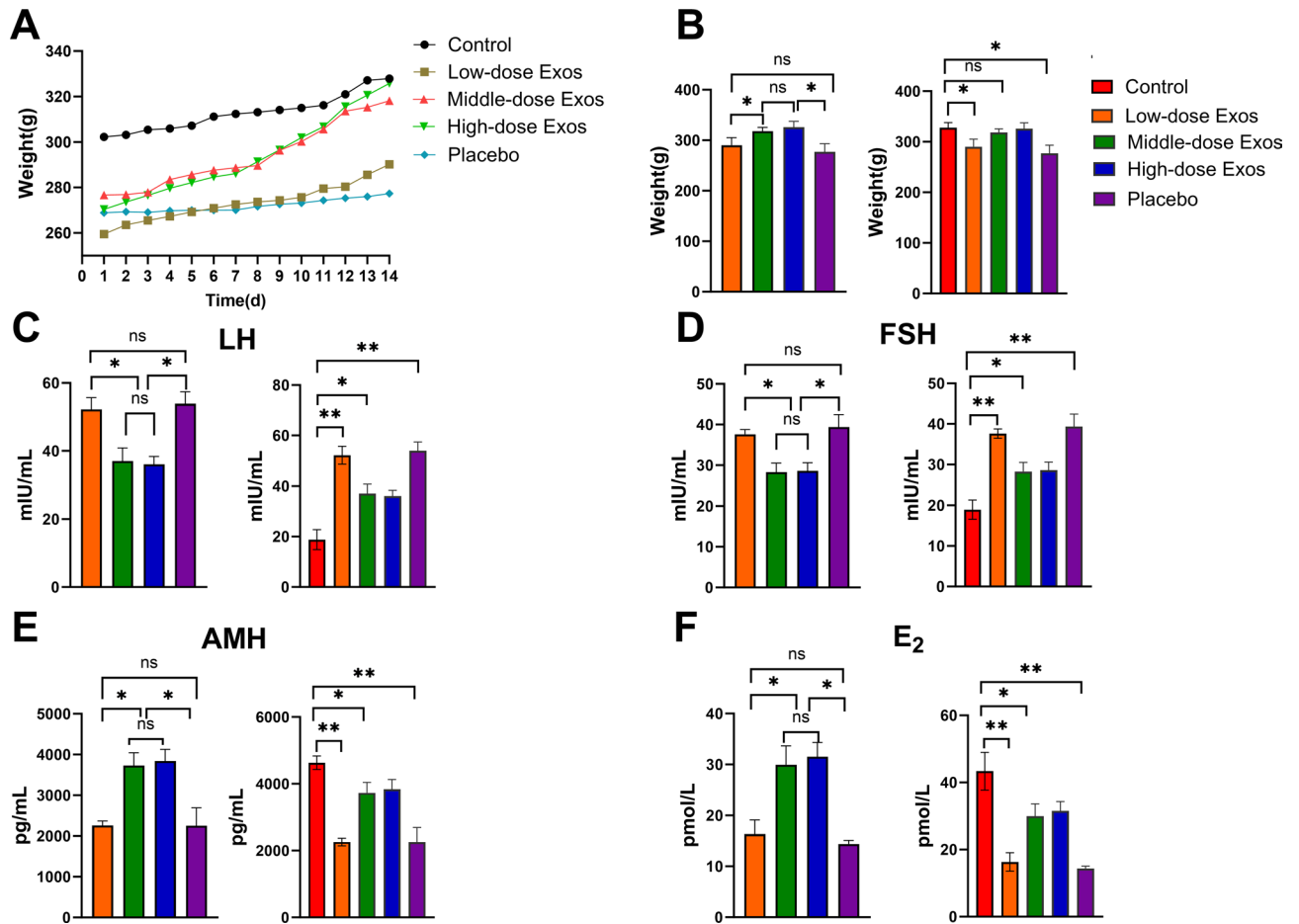


**Fig. 4.** Comparison of weight change and serum sex hormones after MenSCs-Exos transplantation in different groups. **(A):** Trend of weight changes after MenSCs-Exos transplantation in different groups. **(B):** Comparison of weight after MenSCs-Exos transplantation in different groups. **(C)–(F):** Comparison of LH, FSH, AMH and E<sub>2</sub> within and between all groups. Data were represented as mean  $\pm$  SD, \* $P < 0.05$ , \*\* $P < 0.01$ .

possess the same therapeutic potential as their source MSCs<sup>21,22</sup>. They exhibit higher biological stability, better biocompatibility, lower toxicity, and lower immunogenicity compared with MSCs. Furthermore, exosomes can not only protect encapsulated molecules from degradation but also facilitate their cellular uptake via endocytosis<sup>23</sup>. Researches have proposed that exosomes-based therapy is better than MSCs cell therapy in terms of safety, efficacy, and versatility<sup>24</sup>. As a matter of fact, exosomes, secreted by MSCs from different tissues, have gradually been confirmed their therapeutic effects on POF<sup>25,26</sup> and transplantation of exosomes derived from MenSCs could markedly promote follicle development, encourage granulosa cells proliferation, restore ovarian function and fertility in a POI animal model<sup>27</sup>.

Considering the advantages of MenSCs, such as unique proliferative ability, self-renewal characteristics, periodic non-invasive acquisition, abundant availability, easy in vitro isolation and cultivation, no ethical concerns, low cost, low immunogenicity, feasibility of autologous transplantation, and easy large-scale commercial production—MenSCs are considered an ideal source of exosomes for tissue engineering and regenerative medicine. In our study, MenSCs expressed markers which was consistent with previous report<sup>14</sup>. Therefore, MenSCs-Exos hold great promise as a cell-free therapy for treating POF and avoid the disadvantages of MSCs transplantation. In our study, purified MenSCs-Exos were prepared using a patented technology, which ensured their high purity and biological activity, thus supporting their potential for clinical application.

Chemotherapy is a well-known risk factor for POF, so chemotherapy-induced POF rat model was always used to mimic human POF patients<sup>9</sup>. CTX is an alkylating agent usually causing ovarian morphology, oocytes, granulosa cells damaged, ultimately leading to POF<sup>28</sup>. In this study, we established a rat model of POF by intraperitoneal injection of CTX which led to physical condition deteriorated and related hormones levels irregularly changed in rats. Furthermore, CTX intraperitoneal injection also caused histomorphology damage. After that, rats were randomly signed into five groups with different treatments. Results showed that middle-dose and high-dose MenSCs-Exos transplantation could both restore physical condition like estrous cycle and weight gain in POF rats. The disorder female sex hormones were improved in the middle-dose or high-dose MenSCs-Exos groups. Our study also reported that the sex hormone levels are important indicators for the improvement of damaged ovary and ovarian reserve function. Finally, compared to the placebo group, results also suggested

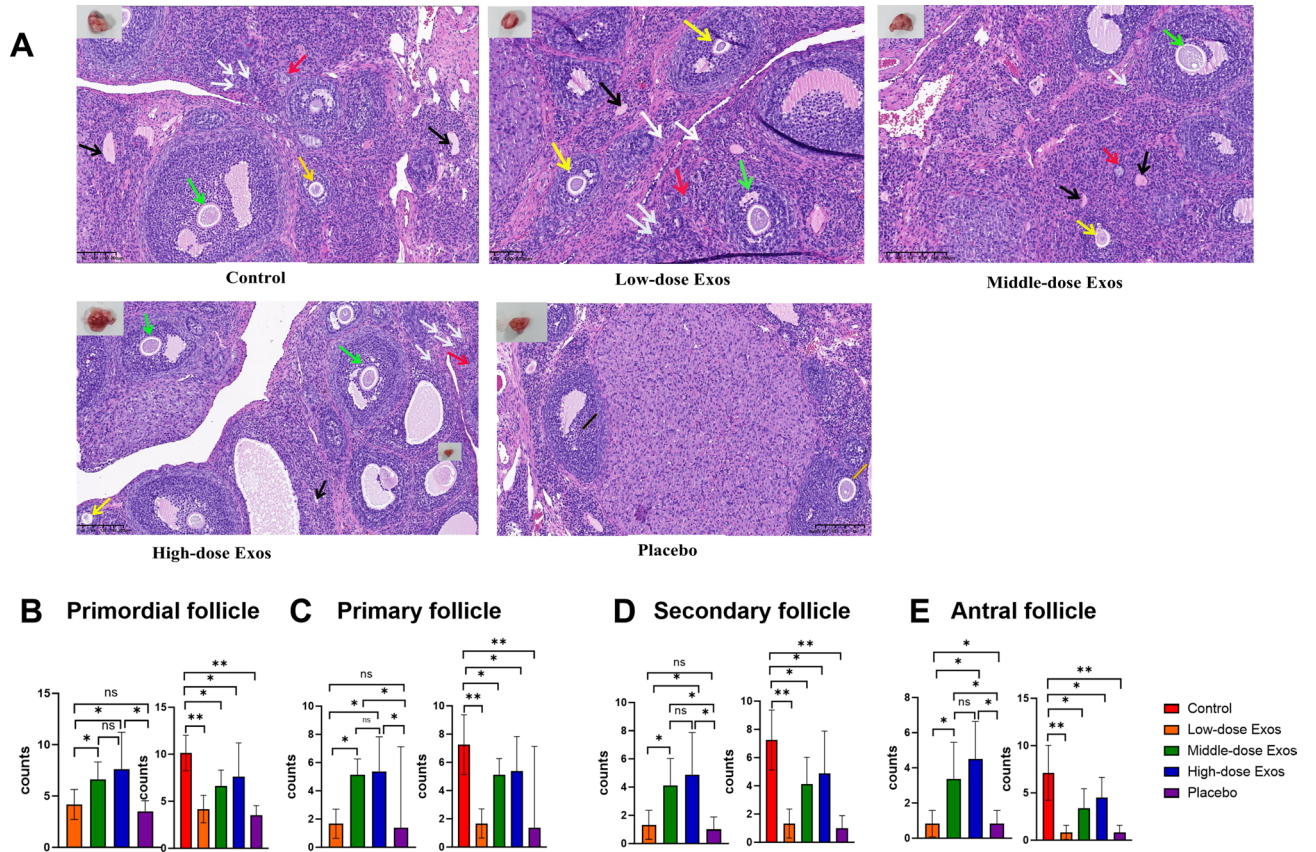


**Fig. 5.** Ovarian morphological, all types of follicles count after MenSCs-Exos transplantation. (A): Morphological changes of ovaries in different groups (scale bar = 100  $\mu$ m) White arrows indicate primordial follicle, red arrows indicate primary follicle, yellow arrow indicate secondary follicle, green arrow indicate antral follicles, and black arrow indicate atresia follicle. (B)–(E): Comparison of all types of follicles counts within and between all groups. Data were represented as mean  $\pm$  SD, \* $P < 0.05$ , \*\* $P < 0.01$ .

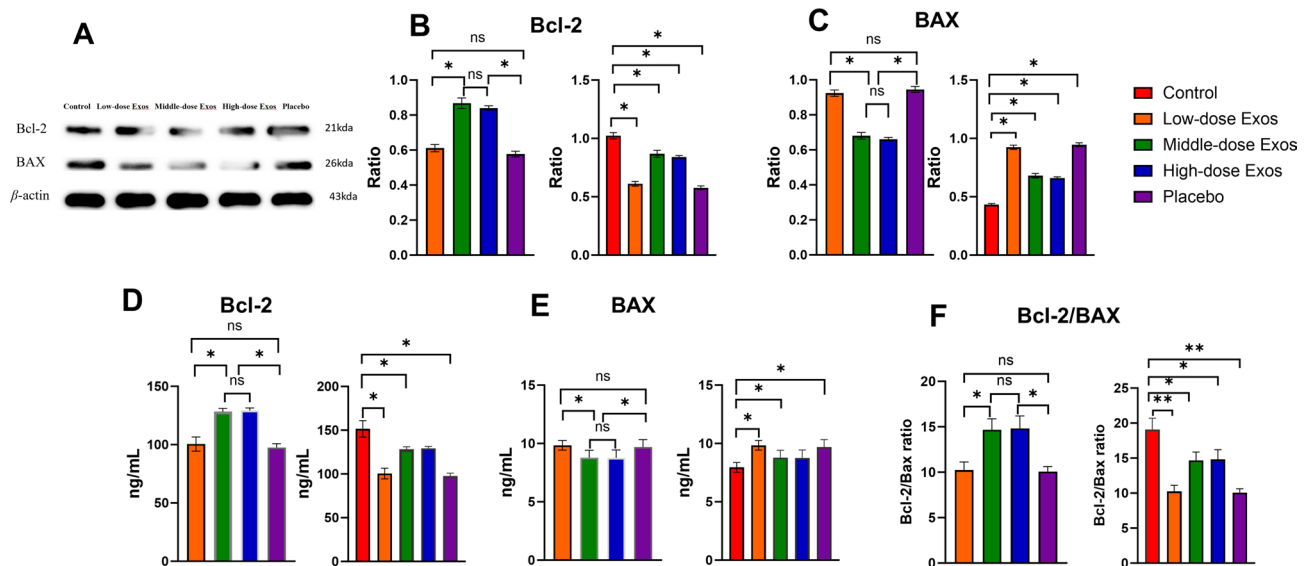


**Fig. 6.** Western blot and ELISA assays of apoptotic-related proteins. (A): Western blot was used to measure the expression of Bcl-2 and Bax in different groups. (B), (C): The relative normalized expression of Bcl-2 and Bax were quantified based on the intensities of the western blot bands. (D), (E): Comparison of Bcl-2 and Bax concentration in ovarian tissue within and between all groups. (F): Comparison of the ratio of Bcl-2 and Bax concentration within and between all groups. Data were represented as mean  $\pm$  SD, \* $P < 0.05$ , \*\* $P < 0.01$ .

that middle-dose or high-dose MenSCs-Exos transplantation significantly repaired damaged ovarian tissues, attenuated ovarian stromal fibrosis, decreased atretic follicles, increased the number of granulosa cells, improved hierarchical arrangement and upregulated the population of follicles in each stage. Our findings are consistent with the work of Yang et al.<sup>13</sup> who demonstrated that bone marrow mesenchymal stem cell derived exosomes transplantation could significantly recover the estrous cycle, increase the number of basal and sinus follicles in POF rats, increase E<sub>2</sub> and AMH levels, and reduce FSH and LH levels. In summary, the novelty of MenSCs-Exos is underscored by their unique source, significant therapeutic potential in treating conditions like POI, potent immunomodulatory effects, and their ability to regulate apoptosis. These characteristics highlight the potential of MenSCs-Exos as a novel and effective therapeutic tool in treating POF.

In order to clarify the mechanism of MenSCs-Exos in repairing the damaged ovarian in POF rats, we detected the expression and concentration of apoptotic-related proteins in rat ovary tissue. Bcl-2 and Bax belong to the Bcl-2 family, which are both important apoptotic-related marker proteins and play a critical part in the apoptosis of the ovarian granulosa cells<sup>29</sup>. It has been reported that Bcl-2 exerts an anti-apoptotic effect by forming heterodimers with Bax. The overexpression of Bcl-2 can antagonize the effect of Bax and inhibit the apoptosis of ovarian granulosa cell<sup>30</sup>. In contrast, Bax protein inhibits the anti-apoptotic effect of Bcl-2 and accelerates the apoptosis of granulosa cells<sup>31</sup>. In our study, MenSCs-Exos transplantation up-regulated the expression of Bcl-2 protein and down-regulated the expression of Bax protein in the middle-dose and high-dose MenSCs-Exos groups. We speculated that MenSCs-Exos transplantation promoted the expression of anti-apoptotic protein BCL-2, while inhibited the expression of pro-apoptotic protein Bax, and then further protect granulosa cells from apoptosis, promote the repairing of damaged tissues in the ovary, and thus ultimately restoring ovarian function and tissue morphology<sup>32</sup>. On the other hand, increased numbers of primary and secondary follicles also suggested that MenSCs-Exos could inhibit the apoptosis of granulosa cells<sup>33</sup>.

Our study demonstrated that MenSCs-Exos transplantation is effective in reversing ovarian function and promoting ovarian tissue regeneration in a chemotherapy induced POF rat model. In the POF model, MenSCs-Exos transplantation restored physical condition, reduced LH and FSH levels, increased AMH and E<sub>2</sub> levels, improved ovarian tissue morphology, increased the number of ovarian follicles. The therapeutic effect of MenSCs-Exos may partially by regulating the expression of apoptotic-related proteins to protect granulosa cells from CTX injury. Moreover, the middle-dose of MenSCs-Exos transplantation achieved optimal therapeutic effect compared with low-dose and high-dose MenSCs-Exos groups. MenSCs-Exos transplantation exhibit therapeutic effect in POF model suggests a promising biological cell-free alternative therapy for the restoration of ovarian function of POF patients in clinical practice. The clinical translation of MenSCs-Exos requires a focus on GMP-grade production methods and clear regulatory pathways to ensure safety, efficacy, and approval for clinical use. A detailed roadmap for the next steps in MenSCs-Exos research should include reproductive outcome testing, long-term fertility follow-up, and biodistribution also. These steps will enhance the impact of MenSCs-Exos and facilitate their clinical translation for the treatment of conditions like premature ovarian failure.

This study has several limitations. First, further studies are needed to investigate the effects of MenSCs-Exos transplantation on the fertility of POF rats. Additionally, delivery route plays crucial role in treatment of POF. Finally, MenSCs-Exos were administered by conventional intravenous injection and their efficacy may be affected due to the certain distance from the target tissue, so the optimal delivery route for MenSCs-Exos transplantation still require further investigation in large animals before clinical application.

## Conclusion

In summary, we demonstrated that MenSCs-Exos transplantation shows great therapeutic potential for restoring ovarian function and ameliorating ovarian pathological damage in a rat POF model. MenSCs-Exos may represent a novel cell-free biological resource for the clinical treatment of female patients with chemotherapy-induced POF. The standardized production of MenSCs-Exos and optimization of clinical parameters (e. g. , therapeutic dose, delivery route, and timing of exosome administration) will accelerate their clinical translation and ensure their therapeutic efficacy in the near future.

## Data availability

The data that support the findings of this study are available from the corresponding author, Zhen-Yu Xu, upon reasonable request.

Received: 25 March 2025; Accepted: 5 March 2026

Published online: 13 March 2026

## References

1. Coulam, C. B., Adamson, S. C. & Annegers, J. F. Incidence of premature ovarian failure. *Obstet. Gynecol.* **67**(4), 604–606 (1986).
2. Jankowska, K. Premature ovarian failure. *Prz. Menopauzalny* **6**(2), 51–56 (2017).
3. Van-Dorp, W. et al. Reproductive function and outcomes in female survivors of childhood, adolescent, and young adult cancer: A review. *J. Clin. Oncol.* **36**(21), 2169–2180 (2018).
4. Hickman, L. C., Llarena, N. C., Valentine, L. N., Liu, X. & Falcone, T. Preservation of gonadal function in women undergoing chemotherapy: A systematic review and meta-analysis of the potential role for gonadotropin-releasing hormone agonists. *J. Assist. Reprod. Genet.* **35**(4), 571–581. <https://doi.org/10.1007/s10815-018-1128-2> (2018).
5. Santamaria, X. et al. Autologous cell therapy with CD133<sup>+</sup> bone marrow-derived stem cells for refractory Asherman's syndrome and endometrial atrophy: A pilot cohort study. *Hum. Reprod.* **31**(5), 1087–1096 (2016).
6. Fu, Y. X., Ji, J., Shan, F., Li, J. & Hu, R. Human mesenchymal stem cell treatment of premature ovarian failure: New challenges and opportunities. *Stem Cell Res. Ther.* **12**(1), 161 (2021).

7. Sheikhsari, G., Aghebati-Maleki, L., Nouri, M., Jadidi-Niaragh, F. & Yousefi, M. Current approaches for the treatment of premature ovarian failure with stem cell therapy. *Biomed. Pharmacother.* **102**, 254–262 (2018).
8. Zafardoust, S. et al. Intraovarian administration of autologous menstrual blood derived-mesenchymal stromal cells in women with premature ovarian failure. *Arch. Med. Res.* **54**(2), 135–144 (2023).
9. Huang-Doran, I., Zhang, C. Y. & Vidal-Puig, A. Extracellular vesicles: Novel mediators of cell communication in metabolic disease. *Trends Endocrinol Meta b* **28**(1), 3–18 (2017).
10. Park, H. S. et al. Comparison of the therapeutic effects between stem cells and exosomes in primary ovarian insufficiency: As promising as cells but different persistency and dosage. *Stem Cell Res. Ther.* **14**(1), 165 (2023).
11. Van Delen, M., Derdelinckx, J., Wouters, K., Nelissen, I. & Cools, N. A systematic review and meta-analysis of clinical trials assessing safety and efficacy of human extracellular vesicle-based therapy. *J. Extracell. Vesicles* **13**(7), e12458. <https://doi.org/10.102/jev2.12458> (2024).
12. Ding, C. et al. Exosomal miRNA-17-5p derived from human umbilical cord mesenchymal stem cells improves ovarian function in premature ovarian insufficiency by regulating SIRT7. *Stem Cells* **38**(9), 1137–1148 (2020).
13. Yang, M. et al. Bone marrow mesenchymal stem cell-derived exosomal miR-144-5p improves rat ovarian function after chemotherapy-induced ovarian failure by targeting PTEN. *Lab. Invest.* **100**(3), 342–352 (2020).
14. Meng, X. et al. Endometrial regenerative cells: A novel stem cell population. *J. Transl. Med.* **5**, 57 (2007).
15. Bozorgmehr, M. et al. Endometrial and menstrual blood mesenchymal stem/stromal cells: Biological properties and clinical application. *Front. Cell Dev. Biol.* **8**, 497 (2020).
16. Chen, Z. et al. Identification of specific markers for human pluripotent stem cell-derived small extracellular vesicles. *J. Extracell. Vesicles.* **13**(2), e12409 (2024).
17. Li, J. et al. *Cistanche deserticola* polysaccharides protect against cyclophosphamide-induced premature ovarian failure in mice by regulating the JAK-STAT pathway. *J. Ethnopharmacol.* **349**, 119971. <https://doi.org/10.1016/j.jep.2025.119971> (2025).
18. Song, D. et al. Human umbilical cord mesenchymal stem cells therapy in cyclophosphamide-induced premature ovarian failure rat model. *Biomed Res Int* **2016**, 2517514 (2016).
19. Zhang, S., Yahaya, B. H., Pan, Y., Liu, Y. & Lin, J. Menstrual blood-derived endometrial stem cell, a unique and promising alternative in the stem cell-based therapy for chemotherapy-induced premature ovarian insufficiency. *Stem Cell Res. Ther.* **14**(1), 327 (2023).
20. Lai, D. et al. Human endometrial mesenchymal stem cells restore ovarian function through improving the renewal of germline stem cells in a mouse model of premature ovarian failure. *J. Transl. Med.* **13**, 155 (2015).
21. Zhang, Z., Shi, C. & Wang, Z. The physiological functions and therapeutic potential of exosomes during the development and treatment of polycystic ovary syndrome. *Front. Physiol.* **14**, 1279469 (2023).
22. Hade, M. D., Suire, C. N. & Suo, Z. Mesenchymal stem cell-derived exosomes: Applications in regenerative medicine. *Cells* **10**(8), 1959 (2021).
23. Bagno, L., Hatzistergos, K. E., Balkan, W. & Hare, J. M. Mesenchymal stem cell-based therapy for cardiovascular disease: Progress and challenges. *Mol. Ther.* **26**(7), 1610–1623 (2018).
24. Vizoso, F. J., Eiro, N., Cid, S., Schneider, J. & Perez-Fernandez, R. Mesenchymal stem cell secretome: Toward cell-free therapeutic strategies in regenerative medicine. *Int. J. Mol. Sci.* **18**(9), 1852 (2017).
25. Zhang, J., Yin, H., Jiang, H., Du, X. & Yang, Z. The protective effects of human umbilical cord mesenchymal stem cell-derived extracellular vesicles on cisplatin-damaged granulosa cells. *Taiwan J. Obstet. Gynecol.* **59**(4), 527–533 (2020).
26. Liu, C. et al. Extracellular vesicles derived from mesenchymal stem cells recover fertility of premature ovarian insufficiency mice and the effects on their offspring. *Cell Transplant* **29**, 963689720923575 (2020).
27. Zhang, S. et al. Concentrated exosomes from menstrual blood-derived stromal cells improves ovarian activity in a rat model of premature ovarian insufficiency. *Stem Cell Res. Ther.* **12**(1), 178 (2021).
28. Plowchalk, D. R. & Mattison, D. R. Reproductive toxicity of cyclophosphamide in the C57BL/6N mouse: 1. Effects on ovarian structure and function. *Reprod. Toxicol.* **6**(5), 411–421 (1992).
29. Sun, Y. et al. 2, 5-Hexanedione induces human ovarian granulosa cell apoptosis through BCL-2, BAX, and CASPASE-3 signaling pathways. *Arch. Toxicol.* **86**(2), 205–215 (2012).
30. Sasson, R. & Amsterdam, A. Stimulation of apoptosis in human granulosa cells from in vitro fertilization patients and its prevention by dexamethasone: Involvement of cell contacts and bcl-2 expression. *J. Clin. Endocrinol. Metab.* **87**(7), 3441–3451 (2002).
31. Liu, Y. et al. Ethanol promotes apoptosis in rat ovarian granulosa cells via the Bcl-2 family dependent intrinsic apoptotic pathway. *Cell Mol Biol (Noisy-le-grand)* **64**(1), 118–125 (2018).
32. Sun, L. et al. Exosomes derived from human umbilical cord mesenchymal stem cells protect against cisplatin-induced ovarian granulosa cell stress and apoptosis in vitro. *Sci. Rep.* **7**(1), 2552 (2017).
33. Liu, M. et al. Small extracellular vesicles derived from embryonic stem cells restore ovarian function of premature ovarian failure through PI3K/AKT signaling pathway. *Stem Cell Res. Ther.* **11**(1), 3 (2020).

## Acknowledgements

We are grateful to Yong He for animal experiment technical guidance.

## Author contributions

All authors contributed to the study conception and design. XY CHENG, YQ W and LC conducted the experiments; ZY XU, LQ YANG and LY XU prepared the exosomes; MJ LIU performed blot and ELISA; TZ conducted HE staining and histological analysis; YY WANG and GH YANG collected and analyzed the data; YG WANG provided technical and writing guidance; XY CHENG and ZY XU prepared the manuscript for publication and reviewed the draft of the manuscript. All authors read and approved the final manuscript.

## Funding

This study was supported by grants from the National Key R&D Program of China grant (No. 2022YFC2304405 and 2022YFA1105603); Zhejiang Provincial Key Research and Development Program (No. 2019C03015); Hangzhou Health Science and Technology Plan Project (No. B20220020); Medical and Health Technology Plan Project in Gongshu District, Hangzhou, Zhejiang Province (No. A202208); Zhejiang Province Traditional Chinese Medicine Technology Plan Project (No. 2023ZL591); the Key laboratory & Women's Hospital, Zhejiang University School of Medicine (No. ZDFY2022-RG-4). The funders played no role in the design and implementation of the study, data analysis, drafting the manuscript or the decision to submit the manuscript for publication.

## Declarations

### Competing interests

The authors declare no competing interests.

### Additional information

**Supplementary Information** The online version contains supplementary material available at <https://doi.org/10.1038/s41598-026-43562-0>.

**Correspondence** and requests for materials should be addressed to L.X. or Z.X.

**Reprints and permissions information** is available at [www.nature.com/reprints](http://www.nature.com/reprints).

**Publisher's note** Springer Nature remains neutral with regard to jurisdictional claims in published maps and institutional affiliations.

**Open Access** This article is licensed under a Creative Commons Attribution-NonCommercial-NoDerivatives 4.0 International License, which permits any non-commercial use, sharing, distribution and reproduction in any medium or format, as long as you give appropriate credit to the original author(s) and the source, provide a link to the Creative Commons licence, and indicate if you modified the licensed material. You do not have permission under this licence to share adapted material derived from this article or parts of it. The images or other third party material in this article are included in the article's Creative Commons licence, unless indicated otherwise in a credit line to the material. If material is not included in the article's Creative Commons licence and your intended use is not permitted by statutory regulation or exceeds the permitted use, you will need to obtain permission directly from the copyright holder. To view a copy of this licence, visit <http://creativecommons.org/licenses/by-nc-nd/4.0/>.

© The Author(s) 2026